**M. Bourogaoui [1] [2,*], H. Berriri [1] H. Ben Attia Sethom [1 2], I. Slama Belkhodja[1]**

J. Electrical Systems 10-2 (2014): 194-208

**Regular paper**

# Encoder Disturbance Fault Detection in PMSM Drives

Journal of Electrical Systems

The paper deals with position sensor fault detection in Permanent Magnet Synchronous Motor (PMSM) drives. Two fault detection algorithms are described here. The first algorithm is based on Discrete Wavelet Transform (DWT) and especially on MultiResolution Analysis (MRA) technique. The second algorithm is based on the Parity Equations Approach (PEA) for residuals generation. The considered position sensor fault is a high level noise disturbance. Simulation results related to the both fault detection algorithms application are presented and discussed. The effectiveness, the robustness to noise, and the real time implementation are the criteria considered to carry out a comparative study between the two fault detection algorithms.

Keywords: Position Sensor Fault, PMSM drive, Fault Detection, Discrete Wavelet Transform, Parity Equations.

## 1. Introduction

Nowadays, modern technological systems need to maintain desirable stability and performance proprieties after faults or failures occurrence. This can be performed thanks to fault tolerant control systems. The advancements made on fault tolerant control systems are particularly important for sensitive systems, such as transportation, aircrafts, propulsion systems and industrial applications. These systems need service continuity especially in closed-loop control operating. In other words, it is a primary purpose to ensure reliability, maintainability and survivability of those systems. That's why, several control systems approach have been designed and developed in order to tolerate faults occurrence.

In addition, such efforts have been made on AC drive applications, particularly induction motors and synchronous motors applications. Recently, a particular interest is given to Permanent Magnet Synchronous Motors (PMSM drives). Indeed, many research results have dealt with fault detection in PMSM drives, but most of them focused on power semiconductors faults and motor faults (stator, rotor, and bearing faults) [1-8].

Thus, PMSM drives control requires the use of position sensors which may be sensitive to faults occurrence such as total or partial loss of the position information, offset, disturbances, measure deviation, channel mismatch, etc. [9-11]. Moreover, these faults lead to dangerous system operation and instability or even to the PMSM drive breakdown. That's why an effective and fast fault detection and isolation must be performed in order to avoid the system hard failure and to reconfigure the PMSM drive control thanks to fault tolerant control strategies [11-15].

Numerous approaches, used for electric drive sensors fault detection and isolation, have been proposed such as fuzzy logic, neural networks, statistical classifiers, signal processing–based techniques (frequency and time – frequency analysis, continuous and discrete wavelet decompositions), parity equations, state estimations or parameters

*Corresponding author: M. Bourogaoui, Université de Tunis El Manar, Ecole Nationale d'Ingénieurs de Tunis, LR11ES15 Laboratoire des Systèmes Electriques, 1002, Tunis, Tunisia, E-mail:manef_bourogaoui_lse@yahoo.fr

[1] Université de Tunis El Manar, Ecole Nationale d'Ingénieurs de Tunis, LR11ES15 Laboratoire des Systèmes Electriques, 1002, Tunis, Tunisia

[2]Université de Carthage, Ecole Supérieure de Technologie et d'Informatique, 2035, Tunis, Tunisia

estimations [14]. Special investigations have been carried out for the detection of current, voltage and dc-link sensor faults such as in [15-18]. However, few researches have concerned mechanical sensors faults that can occur on speed and/or position sensors associated to electric drives, and especially to PMSM drives.

In this paper, two fault detection techniques used for position sensor fault detection are presented and described. The first technique is based on Discrete Wavelet Transform (DWT) and the second one uses Parity Equations Approach (PEA). Indeed, DWT have been largely investigated in electrical and mechanical fault detection occurring in AC electric machines or their associated inverters, [19-21]. Indeed, such signal processing techniques allow transients and signal singularities detection and fault feature extraction. However, their main drawback consists in no standard parameter setting for a given fault detection problem. On the other hand, PEA has been applied for electrical sensors fault detection in DC motors and in variable speed wind systems. However, the classical form of this approach suffers from its system parameters strong dependency.

This paper focuses first on the detection of position sensor fault using the two fault detection techniques. The considered position sensor fault is a high level noise disturbance. A comparative study is then carried out between these two techniques in order to discuss their advantages and drawbacks according to effectiveness, robustness to noise, and real time implementation criteria.

The present research work is presented through four sections. In the second section, simulation results of the PMSM drive operating under faulty conditions are presented. In the third section, the two fault detection techniques principles are presented. In the fourth section, disturbance fault detection using DWT and PEA techniques is analyzed and discussed. Finally, a comparative study between the two fault detection techniques is discussed in order to illustrate their advantages and drawbacks.

## 2. PMSM drive operating under position sensor disturbance conditions

### 2.1 PMSM drive modeling

The PMSM adjustable speed drive consists of PMSM motor, PWM inverter, current sensors, position sensor and a control algorithm based on a Flux Oriented Control (FOC) strategy. This strategy is based on a direct current controller, a quadratic current controller and a speed controller, as seen in Fig.1.

The classical PMSM mathematical model, considered in the synchronous reference frame (d,q), is described by equations (1) to (7).

$$v_{sd} = R_s i_{sd} + L_{sd} \frac{di_{sd}}{dt} - \dot{\theta}_e L_{sq} i_{sq} \tag{1}$$

$$v_{sq} = R_s i_{sq} + L_{sq} \frac{di_{sq}}{dt} + \dot{\theta}_e L_{sd} i_{sd} + \dot{\theta}_e \Psi_f \tag{2}$$

$$\Psi_{sd} = L_{sd} i_{sd} + \Psi_f \tag{3}$$

$$\Psi_{sq} = L_{sq} i_{sq} \tag{4}$$

$$C_{em} = \frac{3}{2} p\left(\left(L_{sd} - L_{sq}\right) i_{sd} i_{sq} + \Psi_f i_{sq}\right) \tag{5}$$

$$\frac{d\omega_e}{dt} = \frac{p}{J}\left(C_{em} - C_r\right) - \frac{f_v}{J}\omega_e \tag{6}$$

$$\frac{d\theta_e}{dt} = \omega_e \tag{7}$$

The PMSM parameters, considered for performing simulations, are given in appendix I.

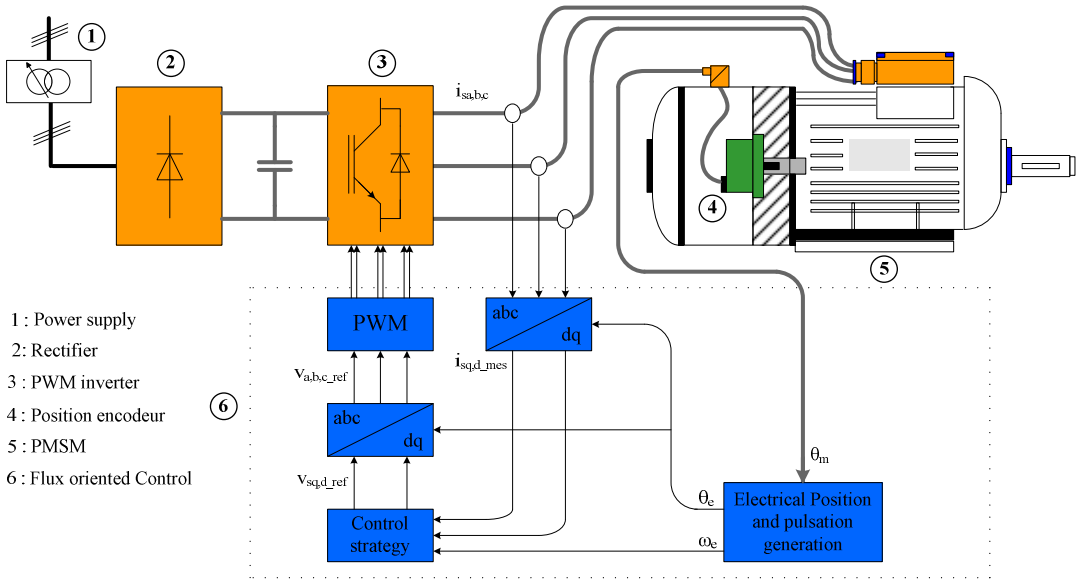


Fig.1. PMSM adjustable speed drive scheme.

## 2.2 Noise sources in PMSM drives

In PMSM drives, several external noise sources can affect sensors in different ways. The main noise source is the electric circuit which can be used with the PMSM drive. For example, in adjustable speed drive applications, inverters are used to drive motors and they are the main source of noise. Indeed, inverters consist of power semiconductors which operate at high and very high switching frequencies [22,23]. In addition, noises are generated through electromagnetic waves or by electric wires which supply converters and motors. That's why; sensors used in PMSM drives may be sensitive to these external noises. Moreover, these noises disturb the measured signals, and it is difficult to eliminate them, which may cause serious and even dangerous consequences on PMSM drives operating when these noises exceed a tolerated level.

## 2.3 Impact of disturbance fault on PMSM drive operating

In this study, the considered position sensor fault is a disturbance of the measured position information by a high level external noise. Indeed, it has been proved in a previous work [10] that a noise level equal or superior to -28dB may distort significantly the supply motor signals and then leads to the instability of the PMSM drive operating.

In order to analyze the position sensor disturbance impact on the PMSM drive operating,

simulation results have been carried out by considering a -28dB noise which has been added arbitrarily to the measured position at a given instant. Moreover, all simulations have been carried out, considering a -50dB level noise added to the PMSM stator current signals, in order to take into account the presence of normal noise level due to a healthy drive operating.

The disturbance occurrence has been considered arbitrarily at $t_d$=0.6s. The rated load torque is applied to the PMSM motor at the instant $t_\ell$=0.4s. Fig.2 shows respectively the phase *a* voltage supply reference $v_{a\_ref}$, the phase *a* stator current $i_{sa}$, the electromagnetic torque $T_{em}$, the mechanical motor speed *N* and the electrical position $\theta_e$, before, during and after the fault occurrence.

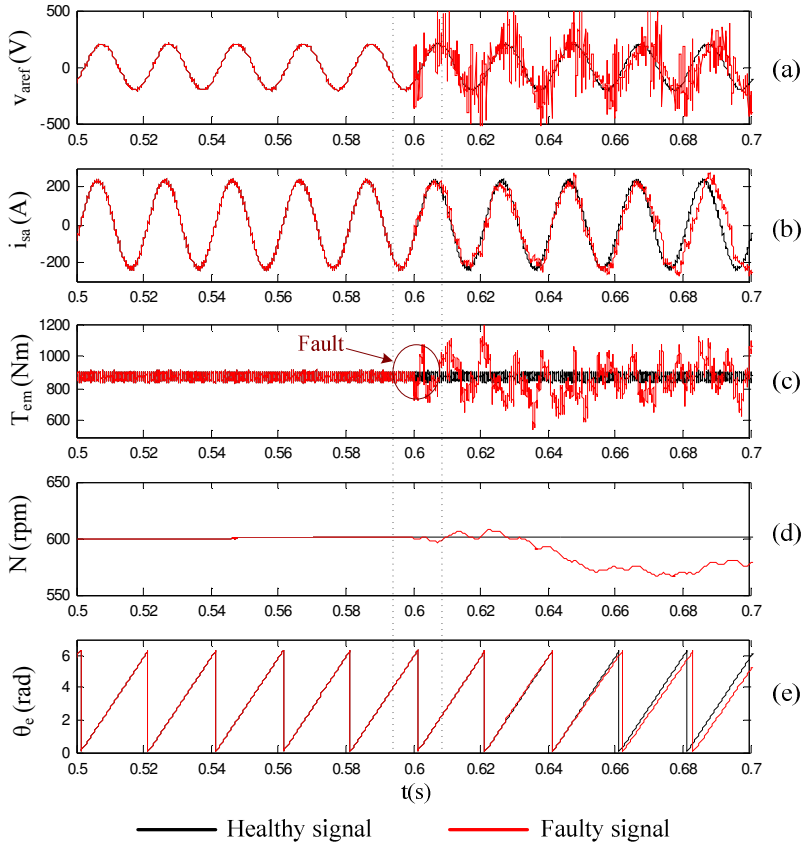


Fig. 2. Position sensor disturbance effects on: (a) voltage supply reference, (b) stator current, (c) electromagnetic torque, (d) mechanical speed and (e) electrical position.

As shown by simulation results of Fig.2, position sensor disturbance has direct consequences on PMSM drive behavior. Indeed, the high level disturbance engenders vibration and even malfunctions in the PMSM drive, which may leads to unsatisfactory performance. Moreover, PMSM drive strategy is based on flux oriented control (FOC) scheme including a speed closed-loop control. Therefore, disturbance fault occurrence affects all control strategy variables. As a first step, and according to the FOC algorithm principle, it affects the speed error which rises dangerously. Consequently, the quadratic current control variable $is_{qref}$ is badly performed. Thus, the disturbance affects the Park transformation matrix which engenders erroneous values of stator voltages references and the PWM inverter is therefore badly controlled.

That's why, after the disturbance occurrence on the position sensor, the PMSM stator currents become distorted and this generates high level harmonics, overheating and high level vibration. On another hand, the speed fluctuation highlights the loss of the motor synchronism.

## 3. The two detection techniques principles

In this study, two detection techniques are considered and used for the detection of the position sensor fault. The first technique is the multiresolution analysis (MRA) based on the discrete wavelet transform (DWT). The second technique is based on the parity equations approach (PEA). The two techniques are presented in Fig.3.

First, DWT-MRA is applied to the PMSM stator current $i_{sa}$, and the residual $Res\_i_{sa}$ is then generated.

Second, PEA is applied to both the electrical position $\theta_e$ and the electrical pulsation $\omega_e$, then two residuals $Res\_\theta_e$ and $Res\_\omega_e$ are respectively generated.

The two techniques principles are presented and discussed in the above subsections.

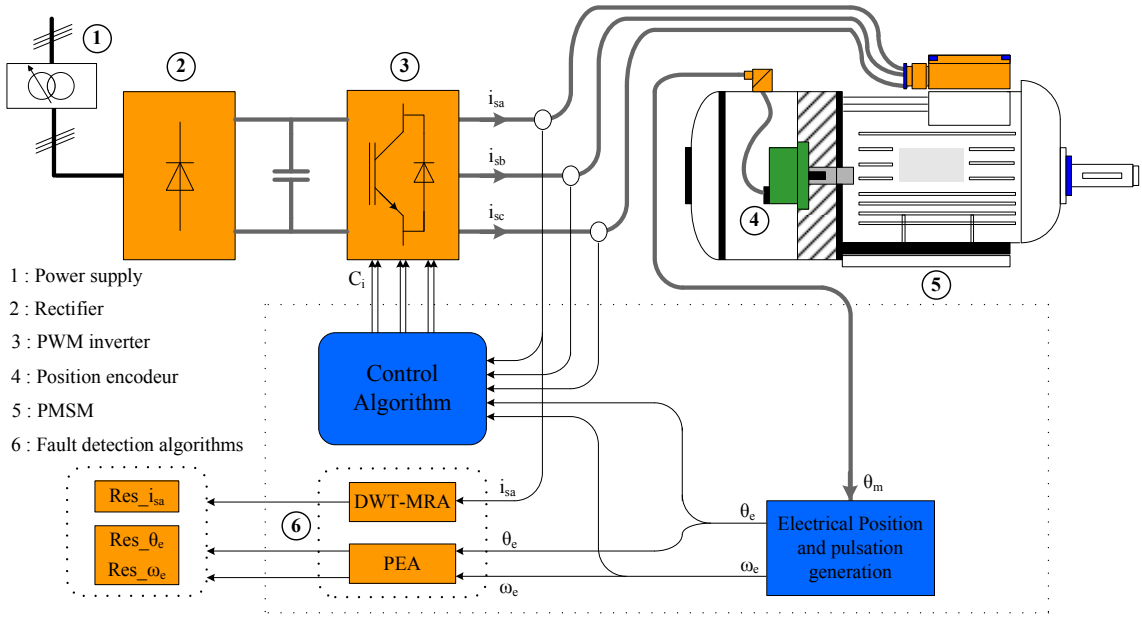


Fig.3. Position sensor fault detection algorithms.

### 3.1. MultiResolution Analysis technique

The MultiResolution Analysis (MRA) algorithm is a DWT – based algorithm using a numerical filter bank, which is composed by low-pass filters (LPF) and high-pass filters (HPF). These filters are used for the construction of the multiresolution time-frequency plane. A fast MRA – based pyramidal algorithm is that of Mallat, which is based on convolution with quadrate mirror filter [24].

The MRA analyzes a numerical signal *S(n)* at many frequency bands with different resolutions by decomposing it into approximations and details information. Indeed, the signal decomposition into different frequency bands is obtained by successive high-pass

$g(n)$ and low-pass $h(n)$ filters. Frequencies contained in the two filters outputs signals are the same as those contained in the input signal, but the data amount is doubled. Consequently, down sampling by a factor 2 is applied to the output of each filter.

Therefore, the detail $d_1$ and approximation $a_1$, which have been given respectively by the high-pass and low-pass filters, can be mathematically expressed as:

$$d_1(n) = \sum_{k=0}^{N-1} s(k)\, g(n-k) \tag{8}$$

$$a_1(n) = \sum_{k=0}^{N-1} s(k)\, h(n-k) \tag{9}$$

Here, $d_1(n)$ and $a_1(n)$ represent the decomposition results at level 1.

The same operation is iterated at the second level of decomposition and it gives $d_2(n)$ and $a_2(n)$ as described by (10) and (11).

$$d_2(n) = \sum_{k=0}^{N/2-1} a_1(k)\, g(n-k) \tag{10}$$

$$a_2(n) = \sum_{k=0}^{N/2-1} a_1(k)\, h(n-k) \tag{11}$$

Thus, the same operation is iterated in order to determine the other decomposition levels depending on the desired level.

Fig.4 illustrates this procedure, where $S(n)$ is the original numerical signal to be decomposed, and $h(n)$ and $g(n)$ are respectively low-pass and high-pass filters.

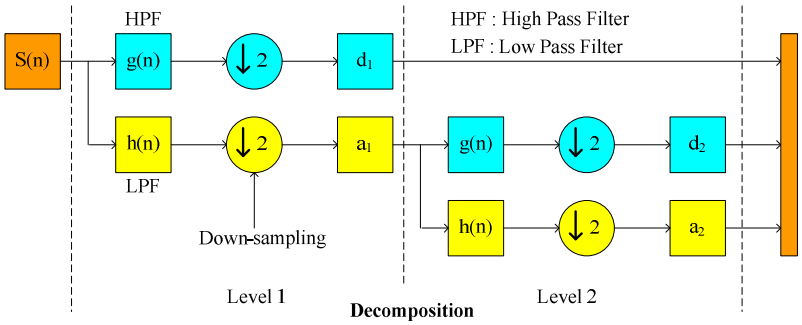


Fig. 4. Two levels S(n) decomposition using MultiResolution Analysis technique principle.

The decomposition of a numerical signal into frequency bands is limited by the samples number $N_s$ of the considered signal. Then the maximum level $J$ depends on the samples number $N_s$. So, the decomposition level $J$ can be determined according to the condition given by the relation (12).

$$2^J \leq N_s \tag{12}$$

The frequency bands limits, relative to approximations and details signals, depend only on the sampling frequency and the decomposition level. Thus, in this work, the sampling frequency is set at $F_e = 10kHz$ and the decomposition level is chosen equal to *7*. Indeed, in the case of this work, this decomposition level is sufficient for highlighting the fault occurrence.

The frequency bands relating to a decomposition level equal to *7* are provided in table 1.

Table 1. Frequency bands related to the stator current decomposition – *J*=7.

| Decomposition level | Frequency bands (Hz) | |
|---|---|---|
| | $a_i$ | $d_i$ |
| 7 | 0 – 39.0625 | 39.0625– 78.125 |
| 6 | 0 – 78.125 | 78.125– 156.25 |
| 5 | 0 – 156.25 | 156.25 – 312.5 |
| 4 | 0 – 312.5 | 312.5 – 625 |
| 3 | 0 – 625 | 625 – 1250 |
| 2 | 0 – 1250 | 1250 – 2500 |
| 1 | 0 – 2500 | 2500 – 5000 |

The decomposition of *S(n)* at the $J^{th}$ level is given by equation (13) [24].

$$S(n) = a_J(n) + \sum_{I=1}^{J} d_I(n) \tag{13}$$

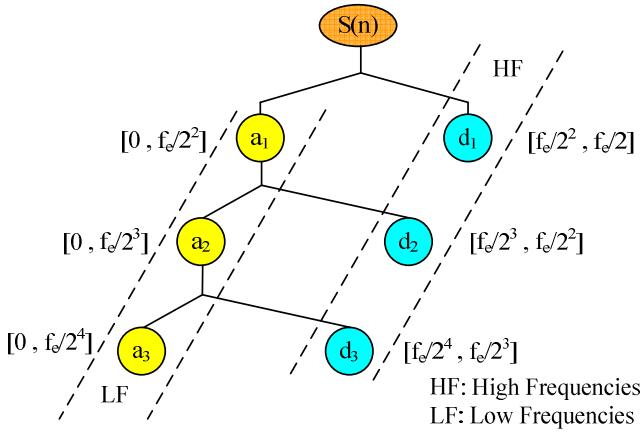


Fig. 5. Frequency bands related to the MultiResolution Analysis of a numerical signal S(n).

Fig.5 highlights the frequency bands related to the approximations and the details obtained from the decomposition of a numerical signal *S(n)* at 3 levels.

The approximation $a_J(n)$ is the product of the approximation coefficients $\alpha_{J,p}$ by the scaling function $\phi_{J,p}$ at level *J*:

$$a_J(n) = \sum_{p=1}^{J} \alpha_{J,p} . \phi_{J,p}(n) \tag{14}$$

where $\phi_{J,p}(n) = 2^{\frac{J}{2}} . \phi(2^J . n - p)$ is the scaling function applied to the scale $2^J$ and shifted by $p$.

The detail $d_I(n)$ is the product of the wavelet coefficients $\beta_{J,p}$ by the wavelet function $\psi_{J,p}$ at each level *I*:

$$d_I(n) = \sum_{p=1}^{I} \beta_{I,p} . \psi_{I,p}(n) \tag{15}$$

where $\psi_{I,p}(n) = 2^{\frac{I}{2}} . \psi(2^I . n - p)$ is the scaling function applied to the scale $2^I$ and shifted by $p$.

### 3.2. Parity Equations Approach and residual generation

Electrical position and electrical pulsation are measured with a short sampling time much lower than the mechanical system dynamic. So, between two consecutive acquisition sampling times, the electrical pulsation remains unchanged. Equation (16) is used for a general formulation of the method.

$$\frac{dx}{dt} = a \tag{16}$$

In this work, equation (7) is considered to apply this formulation where $x = \theta_e$ and $a = \omega_e$.

First order Euler discrete form leads to state equations (17) where the state variable is directly measured and $\xi(k)$ are noises.

$$\begin{aligned} x(k+1) &= x(k) + aT_a \\ y(k) &= x(k) + \xi(k) \end{aligned} \tag{17}$$

In this paper, space parity method is based on measures temporal redundancy in the data window [k, k+2]. Indeed, only three acquisition measurements are performed, for a fast Fault Detection and Isolation (FDI) algorithm. The measures given below by (18) at $k.T_a$, $(k+1).T_a$ and $(k+2).T_a$ instants are derived from (17).

$$\begin{aligned} y(k) &= x(k) + \xi(k) \\ y(k+1) &= x(k) + aT_a + \xi(k+1) \\ y(k+2) &= x(k) + 2aT_a + \xi(k+2) \end{aligned} \tag{18}$$

These measures are arranged using matrices form to apply space parity approach, as it can be seen in [25,26], where the known variables are grouped in one side and the unknown ones ( $x(k)$ and noises) in the other side. A condensed form of (19) is presented in (20).

$$\begin{pmatrix} y(k) \\ y(k+1) \\ y(k+2) \end{pmatrix} - \begin{pmatrix} 0 \\ 1 \\ 2 \end{pmatrix} aT_a = \begin{pmatrix} 1 \\ 1 \\ 1 \end{pmatrix} x(k) + \begin{pmatrix} \xi(k) \\ \xi(k+1) \\ \xi(k+2) \end{pmatrix} \tag{19}$$

$$\boldsymbol{Y}(k,2) - \boldsymbol{G}aT_a = \boldsymbol{H}x(k) + \boldsymbol{\xi}(k,2) \tag{20}$$

where

$$\boldsymbol{Y}(k,2) = \begin{pmatrix} y(k) \\ y(k+1) \\ y(k+2) \end{pmatrix}; \boldsymbol{G} = \begin{pmatrix} 0 \\ 1 \\ 2 \end{pmatrix}; \boldsymbol{H} = \begin{pmatrix} 1 \\ 1 \\ 1 \end{pmatrix}; \qquad \boldsymbol{\xi}(k,2) = \begin{pmatrix} \xi(k) \\ \xi(k+1) \\ \xi(k+2) \end{pmatrix}$$

Parity space methods eliminate the unknown state $x(k)$ using projection technique. A vector $\boldsymbol{V}$, called parity vector, is determined verifying (21).

$$\boldsymbol{V}.\boldsymbol{H} = 0 \tag{21}$$

Many vectors orthogonal to $\boldsymbol{H}$ can be obtained. A simple choice is $\boldsymbol{V} = \begin{pmatrix} 1 & -2 & 1 \end{pmatrix}$. The residual is then calculated by multiplying each side of (20) by this $\boldsymbol{V}$ vector.

$$r(k) = \boldsymbol{V}\left[\boldsymbol{Y}(k,2) - \boldsymbol{G}aT_a\right] = \boldsymbol{V}\,\boldsymbol{\xi}(k,2) \tag{22}$$

The first equality gives the form used for implementation since it depends on known variables, and the second one shows that the residual is null when there is no fault and no noise.

In real conditions, noises always exist, but according to their level in spite of filtering, they can or cannot deteriorate control performances. Then, the residual threshold should be fixed according to these conditions.

Residual equation to be implemented is given by expression (23).

$$r(k) = y(k) - 2y(k+1) + y(k+2) \tag{23}$$

To amplify the residual value, its absolute value is considered. In addition, to confirm the unacceptable noise level, decision is made after three residual computations. So, the final expression of residual, considered for the fault detection, is given by equation (24).

$$R(k) = |r(k)| + |r(k-1)| + |r(k-2)| \tag{24}$$

## 4. Disturbance fault detection using DWT and PEA techniques

In this section, the position information disturbance fault detection is analyzed and discussed using respectively DWT and PEA techniques. The two techniques have been applied to PMSM drive variables obtained from simulations carried out with a sampling rate of 10 kHz which has been considered to perform the PMSM FOC strategy.

### 4.1. Position sensor disturbance detection using DWT technique

It has been shown in a previous work [10] that a 7-level multiresolution analysis decomposition of the PMSM stator current $i_{sa}$ has been sufficient to highlight the disturbance fault occurrence.

In this section, the multiresolution analysis of the stator current has been performed using MATLAB – Simulink®.

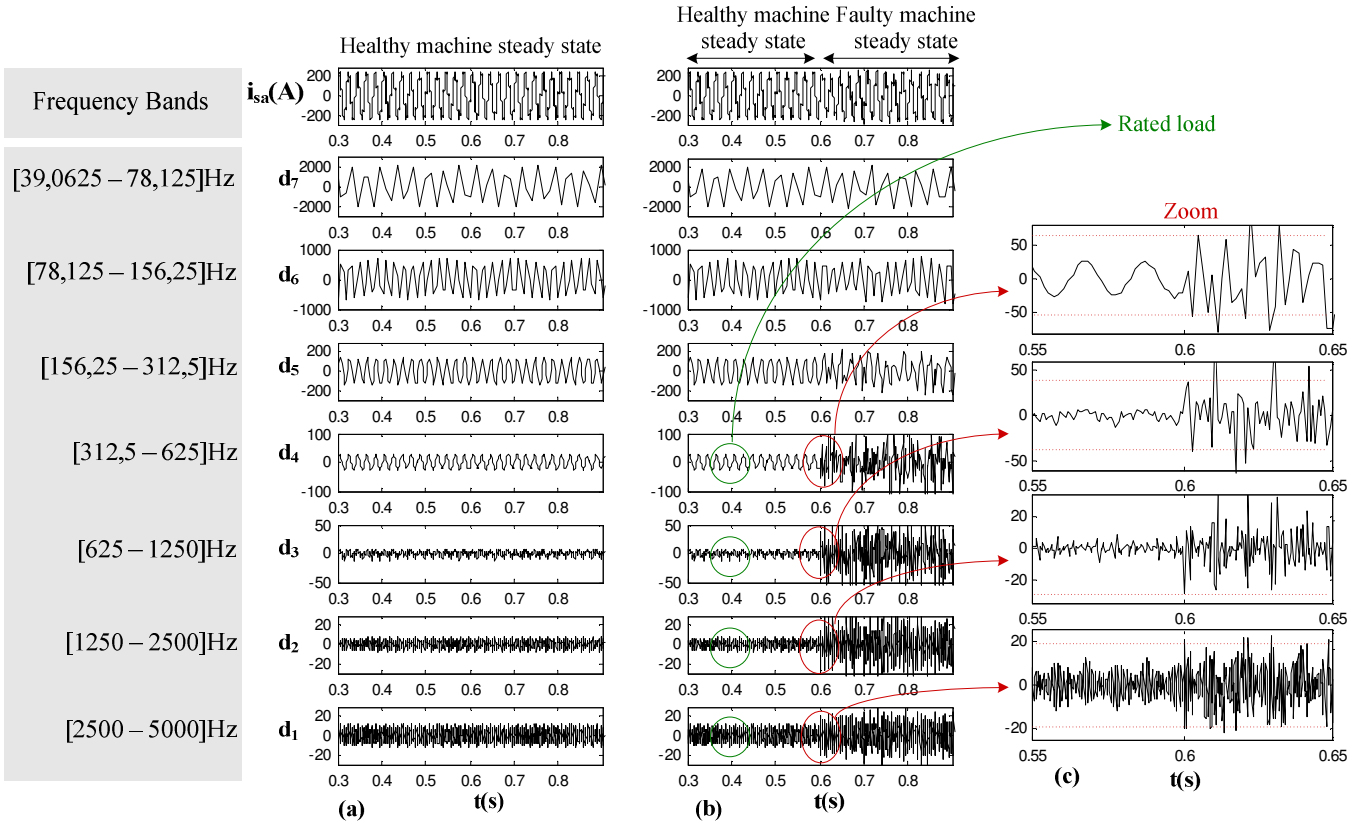


Fig. 6. 7-level multiresolution analysis of $i_{sa}$ using $DB_{10}$,

(a): decomposition in healthy conditions, (b): decomposition in faulty conditions.

Fig. 6 presents 7-level MRA results using the mother wavelet Daubechies noted $DB_{10}$. It illustrates the stator current decomposition into seven details signals respectively in case of healthy conditions operating (a) and in case of faulty conditions operating (b). Thus, it can be noted that there are changes in the details contents, particularly in details $d_1$, $d_2$, $d_3$ and d4, where the disturbance occurrence appears clearly at the instant $t_d$=0.6s.

Fig. 6.c presents a zoom around the fault transient instant in the details signals $d_1$, $d_2$, $d_3$ and $d_4$.

It can be concluded that it is possible to fix detection thresholds related to details $d_1$, $d_2$, $d_3$ and $d_4$ in order to ensure an effective detection of the position sensor disturbance fault occurrence.

On the other hand, Fig. 6 shows clearly that there is no changes in details contents relatively to the load torque application (t=0.4s). Therefore, it can be noted that DWT-MRA technique allows discrimination between transient due to torque condition variation and transient related to disturbance fault occurrence.

### 4.2. Position sensor disturbance detection using PEA technique

The same simulation conditions, considered in subsection 4.1., have been used to carry out the detection of the position sensor fault by applying the PEA – based fault detection algorithm. The method has been applied to generate the position residual $Res\_\theta_e$.

As shown by simulation results of fig.7.a, $Res\_\theta_e$ is sensitive to the position sensor fault occurrence and allows detecting it. Moreover, the low value of the position residual can be amplified to obtain a more significant residual. This can be performed by generating the electrical pulsation residual $Res\_\omega_e$ starting from the principle that the electrical pulsation is derived from the electrical position, as it can be seen in fig.7.b.

In another side, the residual generation algorithm remains not sensitive to load condition variation in the PMSM drive. Then, it can be concluded that PEA allows discrimination between transient due to torque condition variation and transient related to disturbance fault occurrence.

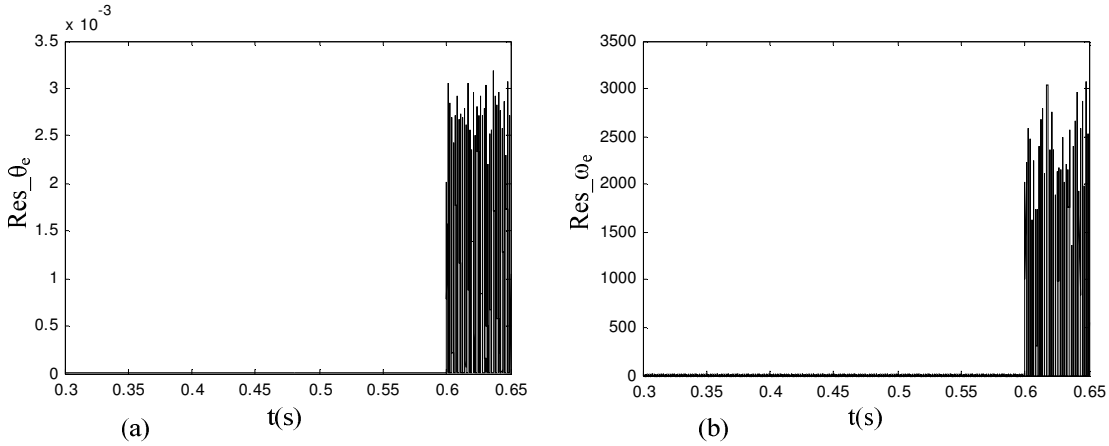


Fig. 7. Position residual (a) and electrical pulsation residual (b) performed for position sensor disturbance detection.

## 5. Discussion

In order to conclude to advantages and drawbacks of each disturbance fault detection algorithm, a comparison between the two detection algorithms is carried out. This comparison is based on effectiveness, robustness and real-time implementation criteria.

As it is known, DWT-MRA algorithm is based on numerical filter banks which necessitate many operations to be implemented. Indeed, expressions (14) and (15) need an important operations number and thus a significant time execution amount to be performed.

Whereas, the residuals generation based on PEA, and as shown by equation (24), necessitates few arithmetical operations to be performed. That's why, real-time implementation of multiresolution analysis algorithm on dsPIC boards is more complicated than that of parity equations algorithm. As a result, PEA based fault detection algorithm is faster than MRA based fault detection algorithm.

In order to illustrate this result, on-line position sensor fault detection has been simulated in Matlab – Simulink® environment for the two fault detection algorithms.

Indeed, Fig.8 shows clearly that the disturbance fault detection results is delayed with respect to the disturbance occurrence. The earlier detection is ensured starting from the detail signal $d_2$ with a delay of 0,4ms.

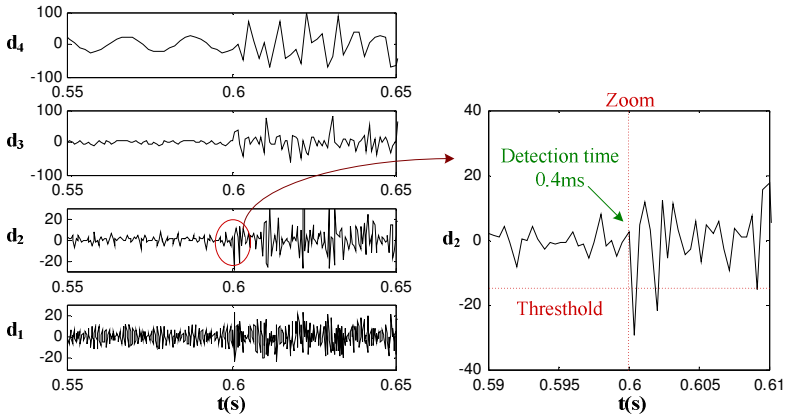


Fig. 8. On-line position sensor fault detection simulation using 7-level MRA of $i_{sa}$

Fig.9 shows clearly that the PEA technique based fault detection can be performed very rapidly within a time period equal to three position measure acquisitions.

On the other hand, simulation results have shown clearly that both detection algorithms are robust to PMSM drive operating normal noise conditions and highlight abnormal occurrence of high level noise disturbance. However, the MRA based detection algorithm parameters setting remains the same for different disturbance levels whereas, the PEA based detection algorithm must be adjusted according to the noise level.

Moreover, both MRA and PEA based detection algorithms allow discrimination between transients related to load variations and transients related to a position sensor fault occurrence, which ensures effective fault detection. Indeed, the rated load torque appliance does not affect neither the detail signals contents nor the position or the electrical pulsation residual.

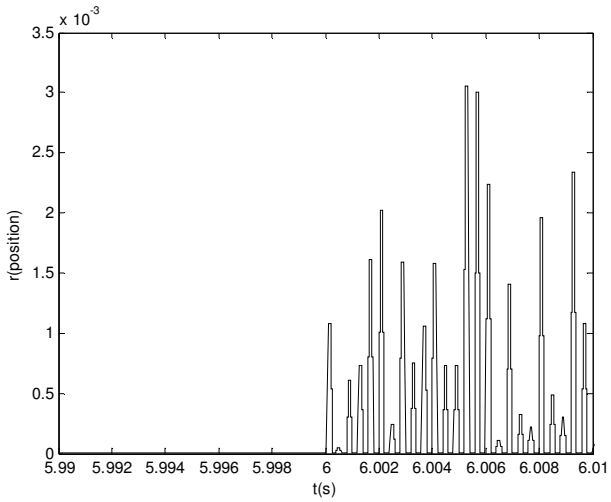


Fig. 9. On - line position sensor fault detection simulation using PEA

Table 2 summarizes the different comparative criteria that were discussed in this section which are effectiveness, rapidness, robustness to noise, simplicity of real time implementation and discrimination between sensor fault and load variation transients.

Table 2. Comparative Criteria of MRA and PEA – based fault detection

| **Criteria** | **MRA – based fault detection** | **PEA – based fault detection** |
|---|---|---|
| Effectiveness | +++ | +++ |
| Rapidness | +-- | +++ |
| Robustness to noise | +++ | ++- |
| Simplicity of real time implementation | +-- | +++ |
| Discrimination between sensor fault and load variation | +++ | +++ |

## 6. Conclusion

In this paper, a comparative study between two fault detection algorithms, used for the detection of PMSM position sensor disturbance fault, has been carried out. The first fault detection algorithm has been based on multiresolution analysis technique. The second fault detection algorithm has concerned the parity equations approach principle.

Simulation results have shown that the two algorithms allow an effective detection of the position sensor disturbance fault and they are robust to normal noise condition operating and load torque disturbance. The advantage of the PEA based detection algorithm is that it provides easy and fast detection of the disturbance fault, whereas the advantage of the MRA based detection algorithm is that its parameters setting remains the same for different disturbance levels.

For future works, the complementarities presented by these two fault detection algorithms can be considered in order to combine them for improving robustness, effectiveness and real time performance of sensor faults detection in electrical drives.

## Acknowledgment

This research project was supported by the Tunisian Ministry of High Education and Scientific Research, under Grant LSE-ENIT-LR11ES15.

## References

[1] A. Gandhi, T. Corrigan & L. Parsa, Recent Advances in Modeling and Online Detection of Stator Interturn Faults in Electrical Motors, IEEE Trans. Ind. Electron, (41), 5, pp. 1564-1575, May 2011.
[2] T.A. Najafabadi, F.R. Salmasi & P.J. Maralani, Detection and Isolation of Speed, DC-link Voltage and Current Sensors Fault based on an Adaptive Observer in Induction Motor Drives', IEEE Trans. Ind. Electron, (58), 5, pp. 1662-1672, May 2011.
[3] T. Benslimane, A New Technique for Simultaneous Detection of one to two Open-Switch Faults in Three Phase Voltage-Inverter-Fed PM Brushless DC Motor Drive, Journal of Electrical Engineering, (58), 2, pp. 97-100, 2008.
[4] M. A. S. K. Khan & M. Rahman, Development and Implementation of a Novel Fault Diagnostic and Protection Technique for IPM Motor Drives, IEEE Trans. Ind. Electron, (56), 1, pp. 85-92, January 2009.
[5] A. Massoum, A. Meroufel, P. Wira & M.K. Fellah, Fuzzy Control of the Permanent Synchronous Machine Singularly Perturbed Fed by a Three Level Inverter, Journal of Electrical Engineering, (63), 3, pp. 186–190, 2012.
[6] K.H. Kim, B.G. Gu & I.S. Jung, Online fault-detecting scheme of an inverter-fed permanent magnet synchronous motor under stator winding shorted turn and inverter switch open, IET Electr. Power Appl., (5), 6, pp. 529–539, July 2011.
[7] S. K. Ahmed, S. Karmakar, M. Mitra & S. Sengupta, Diagnosis of induction motor faults due to broken rotor bar and rotor mass unbalance through discrete wavelet transform of starting current at no-load, J. Electrical Systems, (3), 6, pp 442-456, 2010.
[8] P.J. Rodriguez, A. Belahcen & A. Arkkio, Signatures of electrical faults in the force distribution and vibration pattern of induction motors, IEEE Proc., Electr. Power Appl., (153), 4, pp. 523–529, July 2006.
[9] H. Ben Attia Sethom & M. Bourogaoui, Detection of Position Sensor Default on a Railway Traction PMSM Drive Using Multiresolution Analysis, Proc. Int. Conf. on Ecologic Vehicles and Renewable Energy, Monaco, March 2010.
[10] M. Bourogaoui & H. Ben Attia Sethom, Discrete Wavelet Decomposition Applied to Position Sensor Default Detection on a PMSM Traction Drive, the International Review on Modeling and Simulations IREMOS, (4), 1, Part B, February 2011.
[11] A. Akrad, M. Hilairet & D. Diallo, Design of a Fault-Tolerant Controller Based on Observers for a PMSM Drive, IEEE Trans. Ind. Electron, (58), 4, pp.1416-1427, April 2011.
[12] O. Wallmark, L. Harnefors & O. Carlson, Control Algorithms for a Fault-Tolerant PMSM Drive, IEEE Trans. Ind. Electron, (54), 4, pp. 1973-1980, August 2007.
[13] Y. Zhang & J. Jiang, Bibliographical Review on Reconfigurable Fault–Tolerant Control Systems, Annual Reviews in Control, Elsevier, pp. 229-252, March 2008.
[14] S. Karimi, A. Gaillard, P. Poure & S. Saadate, Current Sensor Fault-Tolerant Control for WECS with DFIG, IEEE Trans. Ind. Electron, (56), pp. 4660-4669, November 2009.
[15] M. Boukhnifer, Active Fault Tolerant Control for Ultrasonic Piezoelectric Motor, Journal of Electrical Engineering, (63), 4, pp 224-232, 2012.
[16] M. Abdellatif, M. Pietrzak-David & I. Slama-Belkhodja, DFIM Vector Control Sensitivity with Current Sensor Faults, The International Journal for Computation and Mathematics in Electrical and Electronic Engineering COMPEL, (29), 1, pp. 139-156, 2010.
[17] I. Bahri, I. Slama-Belkhodja & E. Monmasson, FPGA-Based Real-Time Simulation of Fault Tolerant Current Controllers for Power Electronics, Proc. IEEE Int. Symposium on Ind. Electron. ISIE 2009, Seoul, Korea, pp. 378–383, July 2009.
[18] K. Rothenhagen & F.W. Fuchs, Doubly Fed Induction Generator Model-Based Sensor Fault Detection and Control Loop Reconfiguration, IEEE Trans. Ind. Electron, (56), pp. 4229 – 4238, October 2009.
[19] J.A. Daviu, M.R. Guasp, J.R. Folch, F.M. Gimenez & A. Peris, Application and Optimization of the Discrete Wavelet Transform for the Detection of Broken Rotor Bars in Induction Machines, Applied and Computational Harmonic Analysis, Elsevier, (21), 2, pp. 268-279, September 2006.
[20] G.K. Singh& S.A.S. Kazzaz, Isolation and Identification of Dry Bearing Faults in Induction Machine Using Wavelet Transform, Tribology International, Elsevier, (42), 6, pp. 849-861, June 2009.
[21] M. Aktas & V. Turkmenoglu, Wavelet-based switching faults detection in direct torque control induction motor drives, IET Sci. Meas. Technol., (4), 6, pp. 303–310, November 2010.

[22] K. Gulez, A.A. Adam, I.E. Buzcu & H. Pastaci, Using Passive Filters to Minimize Torque Pulsations and Noises in Surface PMSM Derived Field Oriented Control, Simulation Modeling Practice and Theory, Elsevier, (15), 8, pp. 989-1001, September 2007.
[23] A.A. Adam & K. Gulez, Reduction of Torque Pulsation and Noises in PMSM with Hybrid Filter Topology, Simulation Modeling Practice and Theory, Elsevier, (19), no. 1, pp. 350-361, January 2011.
[24] S. Mallat, A Theory for Multiresolution Signal Decomposition: The Wavelet Representation, IEEE Trans. Pattern Anal. Mach. Intell, (11), 7, pp. 674-693, July 1989.
[25] M. Blanke, M. Kinnaert, J. Lunze & M. Staroswiecki, Diagnosis and Fault-Tolerant Control, Springer, 2003.
[26] H. Berriri, M.W. Naouar & I. Slama-Belkhodja, Easy and Fast Sensor Fault Detection and Isolation Algorithm for Electrical Drives, IEEE Trans. Ind. Electron, pp. 490-499, April 2011.

## Appendix. PMSM parameters

| Variable | Designation | Value |
|---|---|---|
| Rated power | $P_n$ | 53 kW |
| Rated torque | $C_n$ | 852 N.m |
| Rated speed | $N_n$ | 600 rpm |
| Rated current | $I_n$ | 168 A |
| Maximum current | $I_{\max}$ | 368 A |
| Pairs poles Number | $p$ | 5 |